The Journal of Chemical Physics

RESEARCH ARTICLE | MAY 23 2023

Exploring the relationship between softness and excess entropy in glass-forming systems

Ian R. Graham ; Paulo E. Arratia ; Robert A. Riggleman

J. Chem. Phys. 158, 204504 (2023)
https://doi.org/10.1063/5.0143603

AIP Publishing

The Journal of Chemical Physics ARTICLE scitation.org/journal/jcp

Exploring the relationship between softness and excess entropy in glass-forming systems

Cite as: J. Chem. Phys. 158, 204504 (2023); doi: 10.1063/5.0143603
Submitted: 24 January 2023 • Accepted: 25 April 2023 •
Published Online: 23 May 2023

Ian R. Graham,[1] Paulo E. Arratia,[2] and Robert A. Riggleman[3,a)]

AFFILIATIONS

[1] Department of Physics and Astronomy, University of Pennsylvania, Philadelphia, Pennsylvania 19104, USA
[2] Department of Mechanical Engineering and Applied Mechanics, University of Pennsylvania, Philadelphia, Pennsylvania 19104, USA
[3] Department of Chemical and Biomolecular Engineering, University of Pennsylvania, Philadelphia, Pennsylvania 19104, USA

[a)] **Author to whom correspondence should be addressed:** rrig@seas.upenn.edu

ABSTRACT

We explore the relationship between a machine-learned structural quantity (*softness*) and excess entropy in simulations of supercooled liquids. Excess entropy is known to scale well the dynamical properties of liquids, but this quasi-universal scaling is known to breakdown in supercooled and glassy regimes. Using numerical simulations, we test whether a local form of the excess entropy can lead to predictions similar to those made by softness, such as the strong correlation with particles' tendency to rearrange. In addition, we explore leveraging softness to compute excess entropy in the traditional fashion over softness groupings. Our results show that the excess entropy computed over softness-binned groupings is correlated with activation barriers to rearrangement.

I. INTRODUCTION

Despite their importance to numerous technologies, the properties of disordered (amorphous) materials far from equilibrium continue to elude comprehensive understanding.[1–3] Disordered materials made of particulates can span a wide range of length scales, and examples include metallic glasses, nanoparticle packings, colloidal suspensions, foams and emulsions, and granular materials.[4–6] Our knowledge of these materials is primitive compared to our understanding of crystalline solids, where symmetry and order guide detailed theories.[7,8] In disordered systems, the dynamics are known to be strongly heterogeneous and can vary by orders of magnitude even for a supercooled liquid at equilibrium.[9] For many glass-forming systems, the dynamics exhibit a temperature dependence where the activation energy grows upon cooling. Thus, relating the evolution of the material microstructure (at the constituent level) to the material's dynamics (and bulk response) is quite difficult. Much work has been devoted to developing structural indicators of glassy dynamics in disordered systems, with different degrees of success.[10–13] If one is interested in developing thermodynamically consistent coarse-grained and constitutive models, identifying the relevant structural parameters and their connection to thermodynamic quantities is a critical step.[14,15]

In recent years, machine learning (ML) and data science techniques have matured to a point that they are ubiquitous in research and industry. Past studies have successfully applied ML models to predict local dynamical properties of glassy systems more accurately than traditional quantities, such as local potential energy and free volume, for example.[13,16–18] These ML models range in complexity from relatively simple linear support vector machines (SVMs), which operate on vectors of pre-selected structural features for each particle, to convolutional and graph models that are able to extract more intricate spatial correlations within the material and thus lead to improved prediction accuracy on similar tests.[19–22] A notable ML indicator developed to characterize structural defects and predict rearrangements in disordered packings is the quantity known as *softness*.[4,21,23] This quantity was one of the first models developed for glasses and, though relatively simple in its construction from local radial distribution functions, is still able to provide good predictive power.[21,22] The success of machine-learned structural indicators has even motivated the construction of mean-field models that demonstrate the average softness of system is related to the quadratic term of the mean-field potential.[24]

Although *softness* may be more interpretable compared to other machine-learning based models, particles of similar softness still

possess different local structures, complicating its overall physical meaning. For systems in which particles are dominated by isotropic interactions, *softness* can be constructed as a weighted sum of the radial distribution function, where the weights are determined by the SVM. While these weights do inform us to a degree that certain features in the pair correlation function [notably the first and second peaks of $g(r)$] are critical to local dynamics, it remains unknown how the general form of radial weights may be related to *a priori* knowledge of the particles and their interactions. On the other hand, excess entropy, a quantity known to scale with dynamical properties of simple liquids, can be similarly constructed as a simple function of local particle coordinates where deviations in the radial distribution function from that of the ideal gas (a flat distribution) are penalized.[10–12,25,26] Due to the similar construction of these quantities, it is tempting to consider whether there are any connections between them. This would lead to an improved understanding of *softness*, for example. However, one difficulty in such a comparison is that *softness* is defined on a particle basis to strongly correlate with particle-level dynamics, while excess entropy is usually defined for an entire configuration and is associated with system-average dynamics. In this work, we formulate a comparison between these quantities (i.e., excess entropy and *softness*) using two separate approaches. First, we define a local form of excess entropy that takes in a Gaussian-smeared, coarse radial distribution function (similar to *softness*) and compare the ability of this measure to correlate with rearrangements relative to *softness*. Next, we utilize *softness* as an intermediary tool so to compute excess entropy in a more traditional fashion. Essentially, we treat particles of similar *softness* as comprising their own ensembles, allowing us to compute ensemble average quantities (such as excess entropy) over *softness*-grouped subsystems. Our results suggest interesting future directions for combining equilibrium tools with machine-learned quantities in out-of-equilibrium disordered systems.

II. METHODS

A. Simulation details

Numerical simulations comprise sets of equilibrated supercooled states of bidisperse, Lennard-Jones character generated using HOOMD-blue.[27] Configurations are composed of 32 768 particles in a 3D periodic box, and a Nosé–Hoover thermostat is used to integrate the dynamics with a time step of 10^{-3} in the NVT ensemble. We employ a Lennard-Jones potential with a modifiable well-width parameter Δ to control the level of caging in the system; the standard Lennard-Jones definition is obtained when $\Delta = 0.0$. The potential is defined as

$$V_{ij}(r) = \begin{cases} 4\epsilon_{ij}\left[\left(\frac{\sigma'_{ij}}{r-\Delta}\right)^{12} - \left(\frac{\sigma'_{ij}}{r-\Delta}\right)^{6}\right], & r \le 2.5\sigma_{ij}, \\ 0, & r > 2.5\sigma_{ij}, \end{cases} \quad (1)$$

where $\sigma'_{ij} = \sigma_{ij}(1 - \Delta/2^{1/6})$ is defined to keep the minimum at the same position as Δ varies, r is the pair distance between particles, ϵ_{ij} is the interaction energy scale between species i and j, and σ_{ij} is the interaction length scale. The parameter Δ is varied from 0.0 to 0.4, and ϵ_{ij} and σ_{ij} are set in accordance with a standard 80:20 Kob–Andersen-type mixture ($\epsilon_{AA} = 1.0$, $\epsilon_{AB} = 1.5$, $\epsilon_{BB} = 0.5$, $\sigma_{AA} = 1.0$, $\sigma_{AB} = 0.8$, and $\sigma_{BB} = 0.88$). The functional forms are shown in Fig. 1(a) for different choices of Δ. Depending on the value of Δ used, packing fraction ρ is varied between 1.2 and 1.12 to minimize the rapid increase in system pressure p as the well width is decreased. We explored the (Δ, ρ) pairings $[(0.0, 1.2), (0.1, 1.18), (0.2, 1.16), (0.3, 1.14)$, and $(0.4, 1.12)]$. Simulations at $\Delta = 0.5$ were also produced, but they were found to readily crystallize in the supercooled regime; they are omitted from the analysis. We find that by increasing Δ (decreasing the well-width), the fragility is slightly decreased in line with the work of Bordat *et al.*[28] To ensure reproducibility, three randomly seeded replicas were generated for each system. All stated Lennard-Jones units are with respect to the A-species of the standard Kob–Andersen mixture (i.e., $\Delta = 0$). Configurations are initialized on a cubic lattice with random placements of particle species and thermalized well into the liquid regime for each system. The systems are then swept through analyzed temperatures into the supercooled regime, waiting at most 20 τ_α (where τ_α is the alpha relaxation time) at the highest temperature in the supercooled regime and 8 τ_α for the coldest temperature before continuing with the temperate quench. We use the self-intermediate scattering function $(F(\boldsymbol{Q}, t) = \frac{1}{N}\sum_{j=1}^{N} \langle \exp[i\boldsymbol{Q} \cdot (\boldsymbol{r}_j(0) - \boldsymbol{r}_j(t))]\rangle)$ to estimate τ_α by calculating the time required for $F(\boldsymbol{Q}, t)$ to drop below $\frac{1}{e}$. In all systems, we use $|\boldsymbol{Q}| = 7.14$, the wavenumber coinciding with the distance to the first peak of $g(r)$. Furthermore, we apply FIRE minimization as a post-processing step to obtain the inherent structures at each sampled time for final analysis; this step is not strictly necessary to obtain the relationships we find, but serves to remove thermal fluctuations from the analysis.[29] In all parts of the analysis, we explore only the dynamics of A-species particles. We made substantial use of the *freud*, *signac*, and *signac-flow* Python packages to perform post-processing analysis and to manage data and job workflows.[30–32]

B. Softness

As briefly discussed above, *softness* (S) is a machine-learned quantity trained on examples of particles undergoing rearrangement. Here, we closely follow the techniques employed in previous works to construct S in our thermal system.[21,22] We assess whether or not a particle participated in a rearrangement by examining p_{hop}. p_{hop} is defined as

$$p_{hop}(i,t) = \sqrt{\langle (x_i - \langle x_i \rangle_B)^2 \rangle_A \langle (x_i - \langle x_i \rangle_A)^2 \rangle_B}, \quad (2)$$

where x_i is the position of the particle i in simulation, A and B are time intervals defined as $A = [t - t_R/2, t]$ and $B = [t, t + t_R/2]$, and t_R is the time window used. A fairly coarse period is used between frame dumps of $1\tau_A$, where τ_A is the Lennard-Jones time unit in reference to the A species of the $\Delta = 0.0$ system, and we use a time window $t_R = 10\tau_A$. To categorize rearrangements, two cutoffs are defined: $p_H = 0.05$ and $p_S = 0.2$. Particles are deemed *soft* if $p_{hop} > p_S$ and *hard* if $p_{hop} < p_H$. We further restrict our dataset by only processing the peaks and troughs of p_{hop} and asserting that rearrangement events are separated by $10\tau_A$ and non-rearrangements by $80\tau_A$. In case any events are too close, the more prominent peak (or deepest trough) is selected.

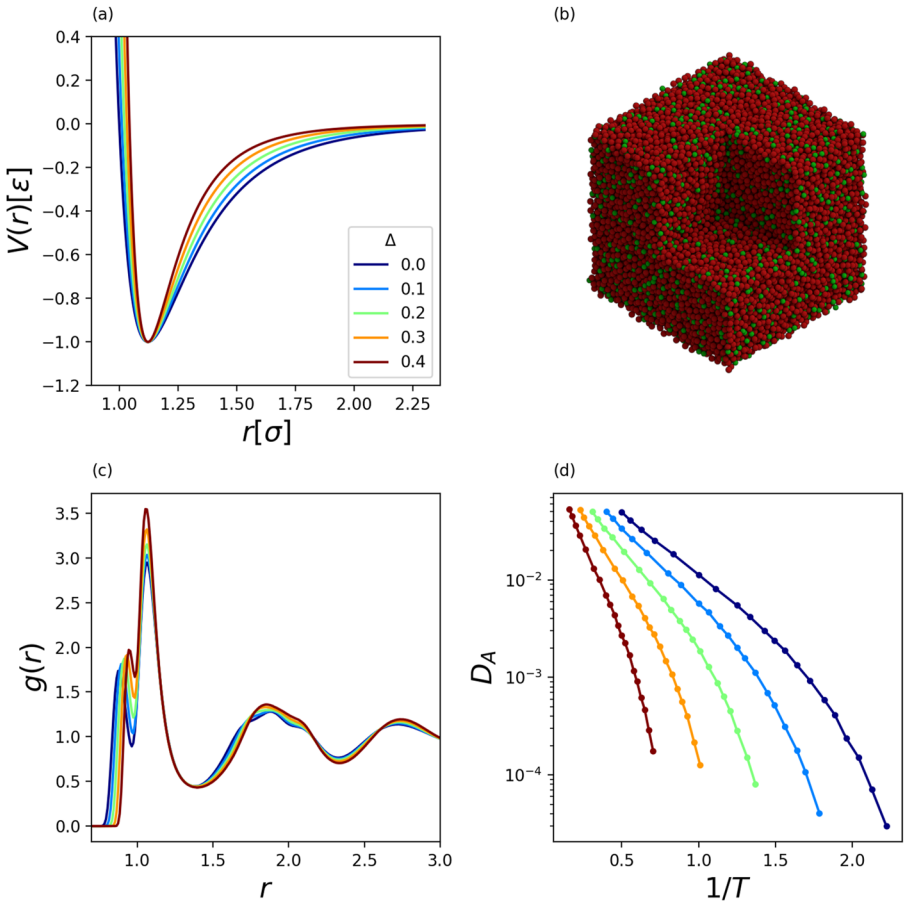

FIG. 1. (a) Pair potentials used in this work. Marginal variation in the Lennard-Jones well width, controlled here by the parameter Δ, leads to significant dynamical changes. (b) Example snapshot of our standard Lennard-Jones Kob–Andersen mixture at $k_BT = 0.45$, $\Delta = 0.0$, produced with the *fresnel* Python library. (c) The total radial distribution functions (RDFs) for the five systems we consider. Higher Δ values lead to a sharpening of RDF peaks, in turn leading to more pronounced caging and slower dynamics at a given temperature. (d) Diffusion coefficients for A species particles measured in both the liquid and supercooled regimes.

Structure functions, $\mathcal{G}_K(\mu_j)$, are calculated from a Gaussian-smeared radial distribution function by using the following equation:

$$\mathcal{G}_K(\mu_j) = \sum_{k\in\{K\}} e^{\frac{(r_k-\mu_j)^2}{2\Delta\mu^2}}, \tag{3}$$

where μ_j is the radial distance of the ith structure function, $\Delta\mu$ is the variance of the gaussian, the label K selects for particle species A or B, and r_j is the radial distance to the particle j. μ_j varies linearly from 0.4 to 3.0 with a step size of $\Delta\mu = 0.1$.[33] With these structure functions, we proceed to train a linear SVM (using the *scikit-learn* package[34]) to classify our soft and hard particles. The final hyperplanes are insensitive to random seeds relating to the SVM optimization and subset of data used. The linear SVM works by finding an optimal hyperplane to separate our classes in the high-dimensional space in which our structure functions reside. Note that we apply a pre-processing step to our data that shifts and scales the structure functions such that within each index pair $(K,\ \mu_j)$ our data have zero mean and unit variance. After fitting the data to our model, we can extract the decision function, which is the signed distance to the hyperplane, and use this measure as our softness S. We find that the accuracy, measured as $P(R|S > 0)$, is between 73% and 80% for the coldest temperatures measured in each system, though this accuracy decreases to 40%–50% at our highest temperatures due to the inherent thermal stochasticity of the liquid state.

C. Excess entropy

Excess entropy, $s^{(2)}$, is classically defined as the difference in configurational entropy between the ideal gas and the system of interest.[11] It can be calculated by a variety of means, including thermodynamic integration.[25] Here, we utilize the simplified and approximate calculation based on the species-dependent radial distribution function $g_K(r)$ as

$$s^{(2)} = -2\pi\sum_K \rho_K \int \left(g_K(r)\log\{g_K(r)\} - g_K(r) + 1\right)r^2 dr \tag{4}$$

in 3D. ρ_K is the density of species K in the sample and r is the radial distance. We additionally construct a per-particle version of $s^{(2)}$ in close analogy to *softness*. The local excess entropy [labeled $s^{(2)}_{loc}$] utilizes the same structure functions as *softness*, but these inputs are

rescaled by the appropriate spherical measure to be transformed back into a coarse, smeared $g_K(r_j)$,

$$g_K(r_j) = (4\pi\rho_K^* r_j^2)^{-1}\mathcal{G}_K(r_j), \tag{5}$$

where ρ_K^* is an effective local density calculated by integrating the RDF for each species, here computed with a sphere of radius $r = 3.0$. From this RDF, we can apply a simple midpoint integration to obtain

$$s_{loc}^{(2)} = -2\pi\sum_K \rho_K^* \sum_j^{j_{max}} [g_K(r_j)\log\{g_K(r_j)\} - g_K(r_j) + 1]r_j^2 L(r_j - \eta)\Delta r, \tag{6}$$

where Δr is the bin width and $L(r_j - \eta)$ is the inverse logistic function centered at a distance of η away. We applied a gentle optimization pass, finding $\eta = 2.0$ to adequately dampen fluctuations at distances at and beyond the second peak of $g(r)$. A few aspects of the form we have chosen here substantially improve the performance of this measure: notably, respecting the bidispersity of the systems and using the local species density ρ_K^*, as opposed to the average system density.

III. RESULTS

A. Comparison of softness and local excess entropy

Here, we examine simulations of a Lennard-Jones Kob–Andersen mixture.[35] We explore four other variations of this system with a modified well width parameter Δ, ranging from 0.0 to 0.4, as shown in Fig. 1(a). Although the modifications to the potential appear subtle, this translates into considerably stronger caging effects within the system and more brittle response overall as Δ is increased.[36] Figures 1(b) and 1(c) show an example snapshot of our Δ = 0.0 system at $k_BT = 0.45$ and samples of $g(r)$ at similar depths into the supercooled regime for each system. The increased caging behavior is reflected in the increased height of the $g(r)$ peaks when Δ is increased. Figure 1(d) shows the diffusion coefficients for these five systems as a function of inverse temperature; particle diffusivity decreases considerably as Δ is increased for the same T.

In Fig. 2, we illustrate how the reduced diffusion coefficient, calculated as $D_A^* = \rho^{\frac{1}{3}}\sqrt{\frac{m}{kT}}D_A$, correlates with both the average softness (S) and excess entropy ($s^{(2)}$) of the systems. The prefactor of the reduced diffusion coefficient originates from Enskog theory, i.e., the kinetics of a dense hard-particle gas.[37] As expected, we observe monotonic behavior in both quantities, but they differ qualitatively in both the liquid and supercooled regimes. In the liquid state, the average S varies little. This is consistent with the understanding that *softness* is well correlated with the effective energy barrier of particles, which should be constant in the liquid regime. As the temperature is decreased below the onset temperature and the average values of S take on a more substantial temperature dependence where S decreases with decreasing T, the relationship between D_A^* and softness changes to a nearly exponential relationship, though the relation is clearly stronger than a simple exponential at the lowest temperatures considered. While these trends are qualitatively similar across different systems, it remains difficult to relate them quantitatively due to the construction of S. This is because S, obtained here as a signed distance from an SVM hyperplane where all dimensions have been rescaled to unit variance over the data distribution, has poorly defined units. In addition, it is a non-trivial issue how one would rescale and shift these dimensions such that particles of a given softness correspond to, for example, the same (reduced) diffusion coefficient from first principles.

For the case of excess entropy in Fig. 2(b), we see expected behavior where in the liquid state the pair approximation of excess entropy does a fair job of estimating reduced diffusion coefficients. However, the trends quantitatively differ once temperatures drop below onset. Application of the three-body term in the excess entropy or its estimation using thermodynamic integration would improve the collapse in the liquid state;[11,25] however, we wish to limit our analysis to predictors that only require a single (or small number) of configurations. Unfortunately, both quantities, S and $s^{(2)}$, fall short as universal predictors of bulk dynamics in the supercooled regime.

Following previous analyses of softness,[21,22] an Arrhenius-like relationship can be found as a function of temperature within the supercooled regime when tracking particles at constant S across

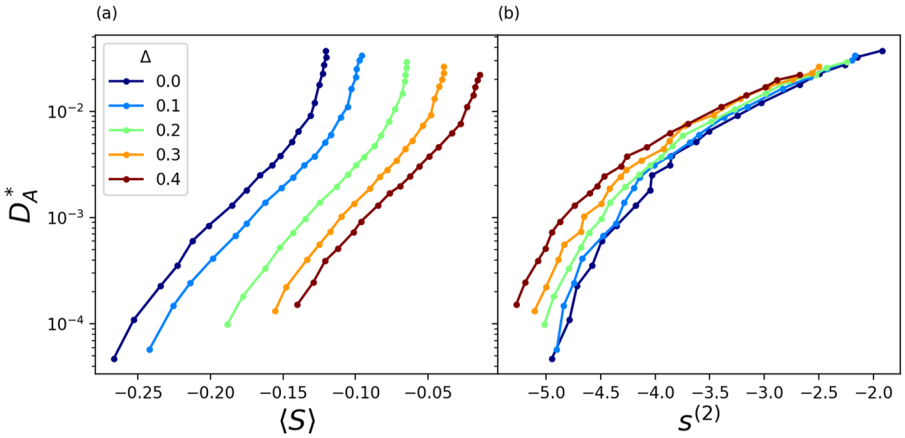

FIG. 2. Reduced diffusion coefficients of the A species as a function of both the average softness (a) and excess entropy (b). $D_A^* = \rho^{\frac{1}{3}}\sqrt{\frac{m}{kT}}D_A$. The behavior of these systems as softness varies, while qualitatively quite similar, fails to agree quantitatively. The results regarding excess entropy, though, depend on the regime. In the liquid state, the excess entropy yields good agreement in the reduced diffusion coefficient across systems, though this breaks down considerably below the crossover temperature.

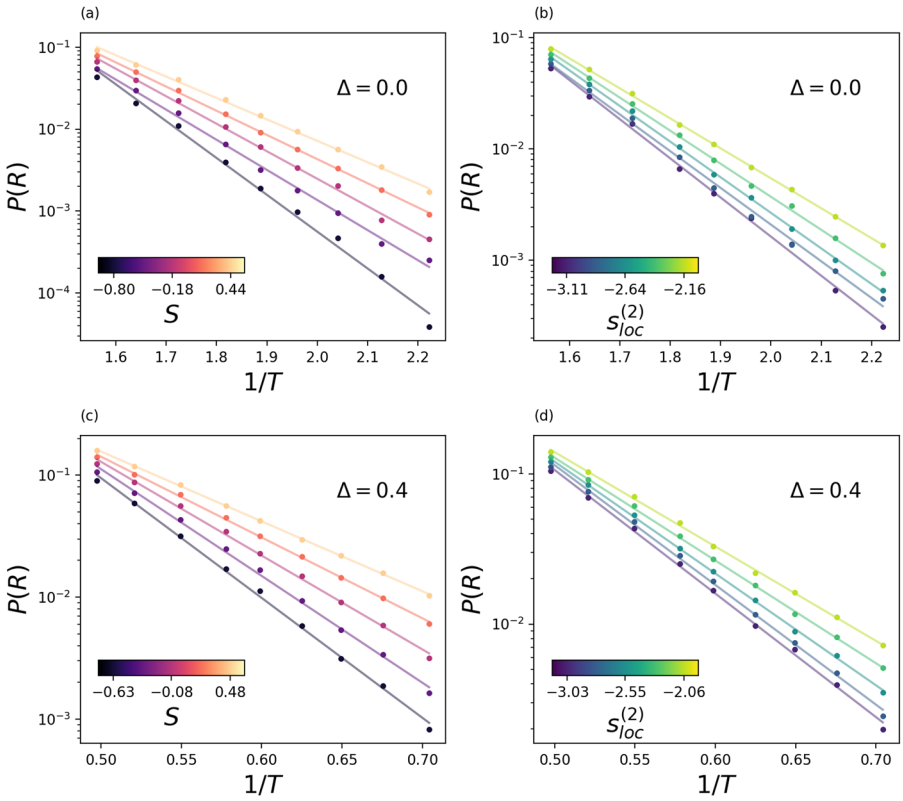

FIG. 3. Probability of rearrangement against inverse temperature across the systems analyzed. Each system is separated into five equally spaced bins of softness, and at each temperature point, we utilize a cutoff in p_{hop} to measure the occurrences of local rearrangements. In (a) and (c), softness is used to group particles with similar dynamics, leading to Arrhenius behavior within each strata. In (b) and (d), we perform the same analysis, but instead using the local excess entropy as our structural proxy for dynamics. Both quantities are able to reproduce Arrhenius behavior within the strata, though softness is more effective in capturing the range of dynamical behavior within the system. The bin-center values of the highest, middle, and lowest bins are marked in the color bar of each subplot.

temperature. In Figs. 3(a) and 3 (c), we show this stratification for the probability of rearrangement in two of our systems binned by *softness*. In each system, we take the 5th and 95th percentile bounds of *softness* and then use five equally spaced bins to aggregate our populations. Furthermore, these Arrhenius fits can be interpreted as relating to the exponential of a free energy barrier of the form $P_R(S) = \exp(\Sigma(S) - \Delta E(S)/T)$, where Σ is the activation entropy, ΔE is the activation energy, and T is the simulation temperature. When viewed this way, effective energetic and entropic barriers can be extracted from the fits, providing a connection between glassy local structures and the characteristic energy barriers governing the system's dynamics.

While these results regarding *softness* are promising, one may wonder if the qualities that we find surprising here (the Arrhenius-like behavior and separation of relaxation rates) are hard to find using other measures of local packing. To explore this issue, we perform a similar analysis using our locally-defined excess entropy, as shown in Figs. 3(b) and 3(d). Although the quantity $s_{loc}^{(2)}$ is not designed specifically to identify rearrangements, one still finds that the local excess entropy exhibits properties similar to those of S. For example, one still obtains good Arrhenius fits to the strata with $s_{loc}^{(2)}$, though the separation of these strata is not as large as with S. Depending on the system, we observe at most an order of magnitude spread in the probability of rearrangement when looking at the coldest temperature sample when applying excess entropy. *Softness*, on the other hand, is capable of extracting an additional order of magnitude or more in this spread.

Next, we directly assess whether excess entropy and softness are correlated with each other. We do so by calculating the Pearson correlation coefficient $\rho_{S,s^{(2)}_{loc}} = \frac{cov(S,s^{(2)}_{loc})}{\sigma_S \sigma_{s^{(2)}_{loc}}}$ between S and $s_{loc}^{(2)}$ as a function of the parameter Δ. Across our systems, we find a moderate correlation, as shown in the inset of Fig. 4(a). We find an increase in the correlation between softness and excess entropy as Δ increases, which appears to plateau at ≈0.5 [Fig. 4(a), inset]. We believe that this is because the tighter well width is increasing the importance of structural entropy on dynamics, though this effect is limited. Softness, in being trained on rearrangement events, is correlated with the free energy barriers to rearrangement and thus captures a combination of both entropic and energetic effects. The lack of energetics in the excess entropy is one possible reason for its poorer performance (in predicting rearrangements) relative to softness.

In addition to predicting local dynamics, analyzing dynamics through softness has also been shown to predict the onset temperature of glassy dynamics, where the dynamics first become super-Arrhenius.[21,38] Here, we replicate the analysis performed by Schoenholz *et al.*[21] to measure the onset temperature from structural heterogeneity, but instead use the local excess entropy. In Fig. 4(b), we show the crossover temperatures estimated from the Arrhenius fits of softness and local excess entropy; the crossover

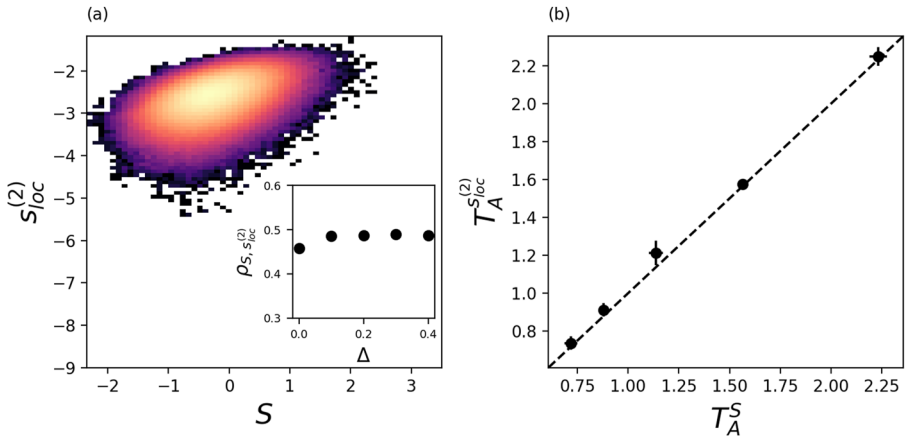

FIG. 4. (a) 2D histogram of softness and local excess entropy at a particle level for the $\Delta = 0.0$ system at $k_BT = 0.47$. (inset) Pearson correlation as a function of Δ. We find a moderate correlation across the systems, which upon closer examination improves with increasing Δ, likely due to the sharpening of the underlying RDF that enters the calculation. (b) Cross-over temperatures estimated from the Arrhenius fits in the supercooled regime using softness and excess entropy. An IQR outlier rejection method is applied to remove poor estimations that occur due to nearly co-linear Arrhenius fits. Values outside twice the 10–90 percentile range (centered on the median) are excluded as likely outliers. Good agreement is found between the estimates using the two quantities.

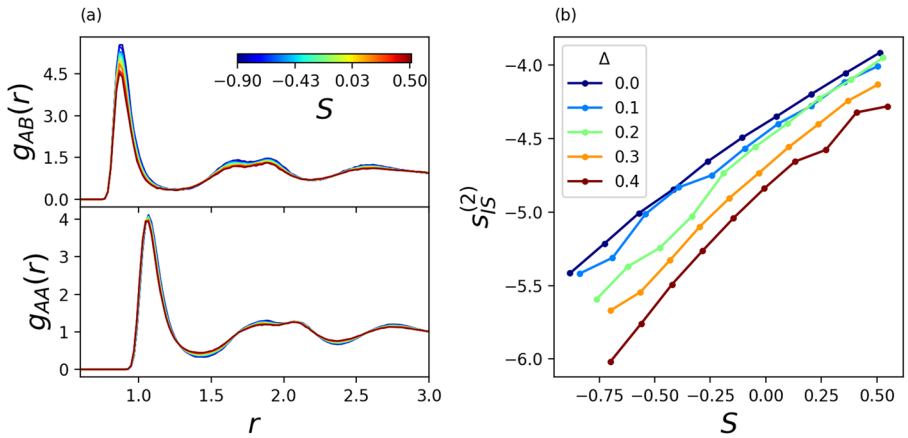

FIG. 5. (a) A–A and A–B radial distribution functions of inherent structures of the $\Delta = 0.0$, $k_BT = 0.49$ system when particles are grouped by softness. Lower-softness inherent structures tend to exhibit enhanced densities of particles at peaks in the RDF and suppression of those within the troughs. (b) Excess entropy computed through inherent structure RDFs of particle groupings with a given softness as a function of the midpoint of the softness bin. The resulting relationship is not quite linear, but monotonically increasing. In Fig. S2 of the supplementary material, we present extended data for $s^{(2)}$ computed from instantaneous trajectories throughout the supercooled regime.

temperatures obtained through the two quantities agree relatively well. This is interesting to note since the traditional methods of extracting a crossover temperature require numerous measurements of long time dynamical quantities, such as the diffusivity, viscosity, or alpha relaxation time. The distinct advantage that we hold by using excess entropy is that it requires no pre-training on data. Thus, local excess entropy appears to be a good and useful structural quantity to determine when the supercooled regime has been entered. We believe that estimating the cross-over temperature from $s^{(2)}_{loc}$ is possible because the structure captured by excess entropy is correlated with short-time dynamical heterogeneities in this regime, though we note that other analyses of excess entropy have been able to extract the onset temperature as well.[39]

One important observation here is that the Arrhenius trend found by softness may not be as unique as previous studies suggest. Instead, the observance of the Arrhenius trend in the supercooled regime may simply hinge on the quantity being at most weakly correlated with rearrangement probability. This also raises concerns about how to validate the performance of softness, in general. Within thermal simulations, we have the freedom to use techniques such as the isoconfigurational ensemble and score our structural quantities by their correlation with propensity or other dynamical quantities averaged over the ensemble.[19,40] However, in athermal

sheared systems, where the rearrangement dynamics are binary in nature, it is difficult to frame softness' effectiveness as a correlation to average per-particle dynamics.

To summarize this section, we find that softness and local excess entropy, although moderately correlated, possess clear differences in their performance that affect their application as local indicators of rearrangement. Softness is clearly more suited to this task, but the moderate correlation suggests that there may be an underlying correspondence between these quantities. It remains that in cases where it is difficult or impossible to compute softness, the local excess entropy may make a fair proxy of dynamical behavior and as a means to estimate the crossover temperature.

B. Building ensembles with softness

Past studies have explored the connection between heterogeneous dynamics of supercooled liquids and thermodynamics by partitioning the system by a measure of the dynamics. For example, in the work of Krekelberg *et al.*,[41] the mean-squared displacement of particles was used to assemble groupings with similar dynamics, and the pair-wise excess entropy was then computed over these groupings. The excess entropy was found to be strongly correlated with the local dynamics, while the average number of neighbors did not correlate. While the mean-squared displacement is a natural choice to perform a grouping like this, other approaches can be considered. In particular, groupings of particles that together display Arrhenius dynamics, and thus well-defined

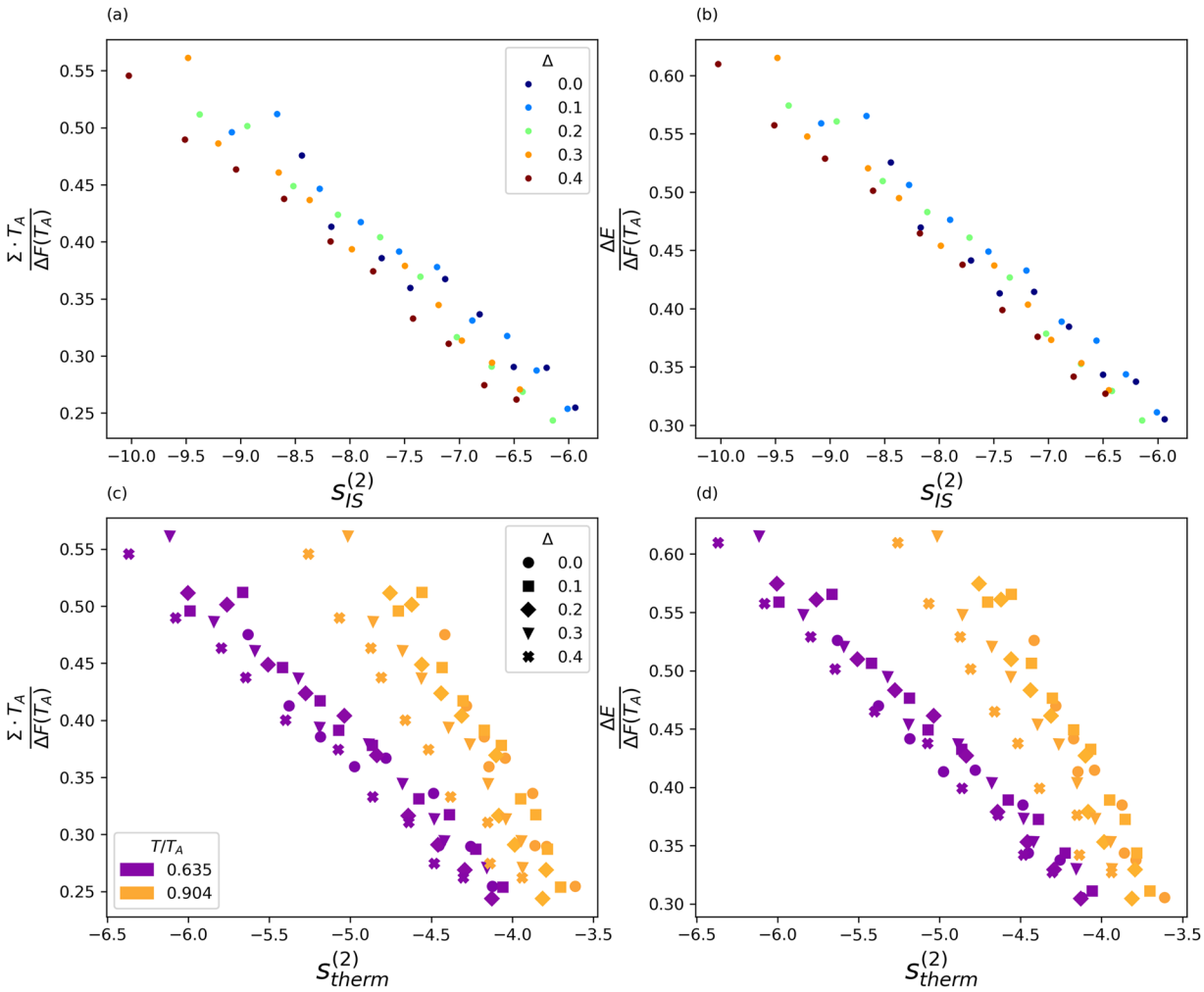

FIG. 6. (a) Entropic and (b) energetic barriers as a function of excess entropy computed from inherent structures. We select similar temperatures relative to onset in each system, though the softness-grouped excess entropies of the inherent structure quenched states are insensitive to temperature. We find that a rescaling by the free energy barrier at onset is sufficient to bring the data into qualitative agreement. In (c) and (d), we show the same barriers, but instead compute the excess entropy from the instantaneous trajectories. Displayed by the color coding are three temperature ratios below onset. The excess entropy computed this way depends on the temperature, but we find similar quantitative agreement in the data when observing the same temperate relative to onset. In Fig. S3 of the supplementary material, we show the extended data for all temperature ranges below onset.

temperature-independent barriers, may be quantitatively related to thermodynamic quantities computed from the average structure of these groupings.

In order gain a deeper insight into the connection between thermodynamics and structure in glassy systems, we propose leveraging the predictive power of machine-learned indicators, such as *softness*, to partition our systems into sub-groupings that possess similar structure and dynamics. Once these groupings are made, we posit that it is appropriate to compute thermodynamic quantities, such as the excess entropy, in the traditional way by averaging over configurations, and that the results of these computations are qualitatively relatable to the actual dynamics. In this way, we propose thinking about the supercooled liquid not as possessing a homogeneous entropy, but as a number of distinct liquid states characterized by a spatially varying entropy, similar to the idea of "entropic droplets" from the random first-order transition theory.[42]

After grouping particles by softness, it is straightforward to construct the radial distribution functions for each group. One common step in analyzing systems using softness is to examine the structure using the inherent structure, which we follow here to remove thermal noise from the positions. When calculating excess entropy on particles grouped by softness, we consider both the inherent structure configurations and the thermal configurations, the latter of which makes a more rigorous connection to the pairwise excess entropy of the liquid. In Fig. 5(a), we show examples of the A–A and A–B radial distribution functions (RDFs) computed from inherent structures. Particles of lower softness possess expected features, with neighbors more highly concentrated at peaks and deficient at troughs. These RDFs are used to compute $s^{(2)}$ as one would for the RDFs of an equilibrated liquid. From this computation, we then have a relation between softness (taken as the midpoint of the softness bin) and excess entropy, as shown in Fig. 5(b). Using the excess entropy at a given softness from Fig. 5(b) and the energy/entropy barriers extracted from Figs. 3(a) and 3(c), we can look for a relationship between the excess entropy and the barriers impeding rearrangements.

In order to compare activation barriers across systems, it is necessary to rescale the barriers by some energy scale related to the activated dynamics. This is because the definition of rearrangement depends on the p_{hop} threshold, which is known to affect the softness-dependent barriers and change across our systems due to the changing well-width of the potential. A natural energy scale to choose is the free energy barrier at onset. In Fig. 6, we show the rescaled entropic and energetic barriers to rearrangement with respect to the excess entropy computed from inherent structures and instantaneous thermal trajectories. We find that excess entropy obtained through both methods leads to qualitative agreement in the rescaled barriers. With the instantaneous trajectories, agreement appears when observing similar temperatures relative to onset. Agreement here suggests that there is a relationship between the liquid excess entropy of softness groupings and the rearrangement barriers that is unaffected by the modifications in potential employed here. It would be interesting in future work to characterize the structure of transition states during glassy rearrangements, as it may provide an insight into the origin of this relationship.

C. Discussion

Our first set of results suggests that quantities such as the local excess entropy are able to recover many of the notable features attributed to softness, e.g., Arrhenius trends in the supercooled regime and an ability to infer the onset temperature for supercooled dynamics. While the overall performance (in terms of predicting particle rearrangements) of excess entropy is not as discriminating as softness, it does well for a quantity that has not been aggressively optimized. Adding enthalpic contributions (even indirectly) could elevate the local excess entropy to an estimate of the *free* energy barrier for rearrangements. A more intricate exploration of the transition states may help to reveal these connections between the local inherent structures and the barriers to rearrangement. Particularly, if one considers ensembles of transition states with the same energy barrier height, what average behavior emerges for the per-particle energies with distance? Is it possible that we could intuit this from a combination of $U(r)$ and its derivatives?

Furthermore, our analysis using softness-grouped ensembles exposes a simple connection between excess entropy and the rearrangement barriers within supercooled liquids. Even though the supercooled state is fraught with many complications due to its rich behavior and metastable nature, there appears to be an optimal partitioning of particles that allows us to make connections to equilibrium thermodynamics. Unfortunately, however, effectively obtaining these groups at the moment requires either dynamical sampling techniques, such as isoconfigurational ensembles, or machine-learned quantities that pose superior correlations with rearrangement dynamics. Quantities derived from low-frequency modes may also be good candidates for this type of aggregation.[17] The framework presented here is a possible path for framing thermodynamics in supercooled liquids, and it may help us to better understand the physical principles responsible for the emergence of glassy behavior at the onset temperature.

SUPPLEMENTARY MATERIAL

See the supplementary material for extended data on the figures above.

ACKNOWLEDGMENTS

This work was funded by the University of Pennsylvania's MRSEC NSF-DMR-1720530.

AUTHOR DECLARATIONS

Conflict of Interest

The authors have no conflicts to disclose.

Author Contributions

Ian R. Graham: Conceptualization (equal); Data curation (equal); Formal analysis (equal); Investigation (equal); Software (equal);

Validation (equal); Visualization (equal); Writing – original draft (equal); Writing – review & editing (equal). **Paulo E. Arratia**: Conceptualization (equal); Funding acquisition (equal); Investigation (equal); Supervision (equal); Writing – review & editing (equal). **Robert A. Riggleman**: Conceptualization (equal); Funding acquisition (equal); Investigation (equal); Supervision (equal); Writing – review & editing (equal).

DATA AVAILABILITY

The data that support the findings of this study are available from the corresponding author upon reasonable request.

REFERENCES

[1]L. Berthier and G. Biroli, "Theoretical perspective on the glass transition and amorphous materials," Rev. Mod. Phys. **83**(2), 587–645 (2011).

[2]P. Charbonneau, J. Kurchan, G. Parisi, P. Urbani, and F. Zamponi, "Glass and jamming transitions: From exact results to finite-dimensional descriptions," Annu. Rev. Condens. Matter Phys. **8**(1), 265–288 (2017).

[3]F. H. Stillinger and P. G. Debenedetti, "Glass transition thermodynamics and kinetics," Annu. Rev. Condens. Matter Phys. **4**(1), 263–285 (2013).

[4]E. D. Cubuk, R. J. S. Ivancic, S. S. Schoenholz, D. J. Strickland, A. Basu, Z. S. Davidson, J. Fontaine, J. L. Hor, Y.-R. Huang, Y. Jiang, N. C. Keim, K. D. Koshigan, J. A. Lefever, T. Liu, X.-G. Ma, D. J. Magagnosc, E. Morrow, C. P. Ortiz, J. M. Rieser, A. Shavit, T. Still, Y. Xu, Y. Zhang, K. N. Nordstrom, P. E. Arratia, R. W. Carpick, D. J. Durian, Z. Fakhraai, D. J. Jerolmack, D. Lee, L. Ju, R. Riggleman, K. T. Turner, A. G. Yodh, D. S. Gianola, and A. J. Liu, "Structure-property relationships from universal signatures of plasticity in disordered solids," Science **358**(6366), 1033–1037 (2017).

[5]D. J. Jerolmack and K. E. Daniels, "Viewing earth's surface as a soft-matter landscape," Nat. Rev. Phys. **1**, 716–730 (2019).

[6]M. van Hecke, "Jamming of soft particles: Geometry, mechanics, scaling and isostaticity," J. Phys.: Condens. Matter **22**(3), 033101 (2009).

[7]A. J. Liu and S. R. Nagel, "The jamming transition and the marginally jammed solid," Annu. Rev. Condens. Matter Phys. **1**(1), 347–369 (2010).

[8]S. Torquato, "Perspective: Basic understanding of condensed phases of matter via packing models," J. Chem. Phys. **149**(2), 020901 (2018).

[9]S. Sastry, P. G. Debenedetti, and F. H. Stillinger, "Signatures of distinct dynamical regimes in the energy landscape of a glass-forming liquid," Nature **393**(6685), 554–557 (1998).

[10]R. T. Bonnecaze, F. Khabaz, L. Mohan, and M. Cloitre, "Excess entropy scaling for soft particle glasses," J. Rheol. **64**(2), 423–431 (2020).

[11]J. C. Dyre, "Perspective: Excess-entropy scaling," J. Chem. Phys. **149**(21), 210901 (2018).

[12]K. Lawrence Galloway, X. Ma, N. C. Keim, D. J. Jerolmack, A. G. Yodh, and P. E. Arratia, "Scaling of relaxation and excess entropy in plastically deformed amorphous solids," Proc. Natl. Acad. Sci. U. S. A. **117**(22), 11887–11893 (2020).

[13]D. Richard, M. Ozawa, S. Patinet, E. Stanifer, B. Shang, S. A. Ridout, B. Xu, G. Zhang, P. K. Morse, J.-L. Barrat, L. Berthier, M. L. Falk, P. Guan, A. J. Liu, K. Martens, S. Sastry, D. Vandembroucq, E. Lerner, and M. L. Manning, "Predicting plasticity in disordered solids from structural indicators," Phys. Rev. Mater. **4**(11), 113609 (2020).

[14]H. C. Öttinger, "Systematic coarse graining: 'Four lessons and a caveat' from nonequilibrium statistical mechanics," MRS Bull. **32**(11), 936–940 (2007).

[15]H. C. Öttinger, H. C. Öttinger, and H. C. Öttinger, *Beyond Equilibrium Thermodynamics* (John Wiley and Sons, Inc., New York, 2005), ISBN: 978-0-471-72791-0, URL http://ebookcentral.proquest.com/lib/upenn-ebooks/detail.action?docID=228475.

[16]R. A. Riggleman, J. F. Douglas, and J. J. de Pablo, "Tuning polymer melt fragility with antiplasticizer additives," J. Chem. Phys. **126**(23), 234903 (2007).

[17]H. Tong and N. Xu, "Order parameter for structural heterogeneity in disordered solids," Phys. Rev. E **90**(1), 010401 (2014).

[18]A. Widmer-Cooper and P. Harrowell, "Free volume cannot explain the spatial heterogeneity of Debye–Waller factors in a glass-forming binary alloy," J. Non-Cryst. Solids **352**(42–49), 5098–5102 (2006).

[19]V. Bapst, T. Keck, A. Grabska-Barwińska, C. Donner, E. D. Cubuk, S. S. Schoenholz, A. Obika, A. W. R. Nelson, T. Back, D. Hassabis, and P. Kohli, "Unveiling the predictive power of static structure in glassy systems," Nat. Phys. **16**(4), 448–454 (2020).

[20]Z. Fan and E. Ma, "Predicting orientation-dependent plastic susceptibility from static structure in amorphous solids via deep learning," Nat. Commun. **12**(1), 1506 (2021).

[21]S. S. Schoenholz, E. D. Cubuk, D. M. Sussman, E. Kaxiras, and A. J. Liu, "A structural approach to relaxation in glassy liquids," Nat. Phys. **12**(5), 469–471 (2016).

[22]S. S. Schoenholz, E. D. Cubuk, E. Kaxiras, and A. J. Liu, "Relationship between local structure and relaxation in out-of-equilibrium glassy systems," Proc. Natl. Acad. Sci. U. S. A. **114**(2), 263–267 (2017).

[23]E. D. Cubuk, S. S. Schoenholz, E. Kaxiras, and A. J. Liu, "Structural properties of defects in glassy liquids," J. Phys. Chem. B **120**(26), 6139–6146 (2016).

[24]M. K. Nandi and S. M. Bhattacharyya, "Microscopic theory of softness in supercooled liquids," Phys. Rev. Lett. **126**(20), 208001 (2021).

[25]I. H. Bell, J. C. Dyre, and T. S. Ingebrigtsen, "Excess-entropy scaling in supercooled binary mixtures," Nat. Commun. **11**(1), 4300 (2020).

[26]X. Ma, J. Liu, Y. Zhang, P. Habdas, and A. G. Yodh, "Excess entropy and long-time diffusion in colloidal fluids with short-range interparticle attraction," J. Chem. Phys. **150**(14), 144907 (2019).

[27]J. A. Anderson, J. Glaser, and S. C. Glotzer, "HOOMD-blue: A Python package for high-performance molecular dynamics and hard particle Monte Carlo simulations," Comput. Mater. Sci. **173**, 109363 (2020).

[28]P. Bordat, F. Affouard, M. Descamps, and K. L. Ngai, "Does the interaction potential determine both the fragility of a liquid and the vibrational properties of its glassy state?," Phys. Rev. Lett. **93**(10), 105502 (2004).

[29]E. Bitzek, P. Koskinen, F. Gähler, M. Moseler, and P. Gumbsch, "Structural relaxation made simple," Phys. Rev. Lett. **97**(17), 170201 (2006).

[30]C. S. Adorf, P. M. Dodd, V. Ramasubramani, and S. C. Glotzer, "Simple data and workflow management with the signac framework," Comput. Mater. Sci. **146**, 220–229 (2018).

[31]V. Ramasubramani, C. Adorf, D. Paul, D. Bradley, and S. Glotzer, "signac: A Python framework for data and workflow management," in *Proceedings of the 17th Python in Science Conference* (2018), pp. 152–159; available at https://conference.scipy.org/proceedings/scipy2018/vyas_ramasubramani.html.

[32]V. Ramasubramani, B. D. Dice, E. S. Harper, M. P. Spellings, J. A. Anderson, and S. C. G. freud, "A software suite for high throughput analysis of particle simulation data," Comput. Phys. Commun. **254**, 107275 (2020).

[33]J. Behler and M. Parrinello, "Generalized neural-network representation of high-dimensional potential-energy surfaces," Phys. Rev. Lett. **98**(14), 146401 (2007).

[34]F. Pedregosa, G. Varoquaux, A. Gramfort, V. Michel, T. Bertrand, O. Grisel, M. Blondel, P. Peter, R. Weiss, D. Vincent, J. Vanderplas, A. Passos, and D. Cournapeau, Scikit-learn: Machine Learning in Python, MACHINE LEARNING IN PYTHON, p. 6.

[35]K. Walter and H. C. Andersen, "Scaling behavior in the β-relaxation regime of a supercooled Lennard–Jones mixture," Phys. Rev. Lett. **73**(10), 1376–1379 (1994).

[36]E. Y. Lin and R. A. Riggleman, "Distinguishing failure modes in oligomeric polymer nanopillars," Soft Matter **15**(32), 6589–6595 (2019).

[37]M. Dzugutov, "A universal scaling law for atomic diffusion in condensed matter," Nature **381**(6578), 137–139 (1996).

[38]A. S. Keys, L. O. Hedges, P. Juan Garrahan, S. C. Glotzer, and D. Chandler, "Excitations are localized and relaxation is hierarchical in glass-forming liquids," Phys. Rev. X **1**(2), 021013 (2011).

[39] A. Banerjee, M. K. Nandi, S. Sastry, and S. M. Bhattacharyya, "Determination of onset temperature from the entropy for fragile to strong liquids," J. Chem. Phys. **147**(2), 024504 (2017).
[40] A. Widmer-Cooper and P. Harrowell, "Predicting the long-time dynamic heterogeneity in a supercooled liquid on the basis of short-time heterogeneities," Phys. Rev. Lett. **96**(18), 185701 (2006).
[41] W. P. Krekelberg, V. Ganesan, and T. M. Truskett, "Structural signatures of mobility on intermediate time scales in a supercooled fluid," J. Chem. Phys. **132**(18), 184503 (2010).
[42] T. R. Kirkpatrick and P. G. Wolynes, "Stable and metastable states in mean-field Potts and structural glasses," Phys. Rev. B **36**(16), 8552–8564 (1987).